Utilizing (p,d) and (p,t) reactions to obtain (n,f) cross sections in uranium nuclei via the surrogate-ratio method

R. O. Hughes,[1,*] C. W. Beausang,[1] T. J. Ross,[1,4] J. T. Harke,[2] N. D. Scielzo,[2] M. S. Basunia,[3] C. M. Campbell,[3] R. J. Casperson,[2] H. L. Crawford,[3] J. E. Escher,[2] J. Munson,[3] L. W. Phair,[3] and J. J. Ressler[2]

[1]*Department of Physics, University of Richmond, 28 Westhampton Way, Richmond, Virginia 23173, USA*

[2]*Lawrence Livermore National Laboratory, Livermore, California 94551, USA*

[3]*Lawrence Berkeley National Laboratory, Berkeley, California 94720, USA*

[4]*Department of Physics, University of Surrey, Guildford GU2 7XH, United Kingdom*

(Received 20 December 2011; published 21 February 2012)

The surrogate ratio method has been tested for (p, d) and (p, t) reactions on uranium nuclei. ^{236}U and ^{238}U targets were bombarded with 28-MeV protons and the light ion recoils and fission fragments were detected using the Silicon Telescope Array for Reaction Studies detector array at the 88-Inch Cyclotron at Lawrence Berkeley National Laboratory. The (p,df) reaction channels on ^{236}U and ^{238}U targets were used as a surrogate to determine the $\sigma[^{236}\mathrm{U}(n,f)]/\sigma[^{234}\mathrm{U}(n,f)]$ cross-section ratio. The (p,tf) reaction channels were also measured with the same targets as a surrogate for the $\sigma[^{235}\mathrm{U}(n,f)]/\sigma[(^{233}\mathrm{U}(n,f)]$ ratio. For the (p,df) and (p,tf) surrogate measurements, there is good agreement with accepted (n,f) values over equivalent neutron energy ranges of $E_n = 0$–7 MeV and $E_n = 0$–5.5 MeV, respectively. An internal surrogate ratio method comparing the (p, d) and (p,t) reaction channels on a single target is also discussed. The $\sigma[^{234}\mathrm{U}(n,f)]/\sigma[^{233}\mathrm{U}(n,f)]$ and $\sigma[^{236}\mathrm{U}(n,f)]/\sigma[^{235}\mathrm{U}(n,f)]$ cross-section ratios are extracted using this method for the ^{236}U and ^{238}U targets, respectively. The resulting fission cross-section ratios show relatively good agreement with accepted values up to $E_n \sim 5$ MeV.

DOI: 10.1103/PhysRevC.85.024613 PACS number(s): 24.87.+y, 24.75.+i, 25.85.Ge, 25.55.Hp

I. INTRODUCTION

Over the past few years the surrogate method, first employed in 1970 [1,2], has emerged as an effective means of indirectly measuring neutron-induced fission cross sections [3–12]. The method can, in principle, be used to determine neutron-induced fission cross sections for unstable nuclei which would otherwise be difficult or even impossible to measure directly due to the requirement of a radioactive target and high neutron flux. The surrogate method has important applications, for example, in determining neutron-induced fission cross sections associated with unstable minor actinide isotopes relevant to fast neutron reactors [12].

Surrogate reactions use a stable beam and target combination to populate the same compound nucleus (CN) as that formed in a neutron-induced reaction of interest. In order to extract $\sigma(n,f)$ values, the fission probability of the CN is measured directly in the surrogate experiment, while the cross section for the incident neutron reaction is calculated from theory. The technique relies on the assumptions that the CN decay is independent of the entrance channel and that the CN is formed at similar spins and excitation energies as in the neutron-induced reaction.

Before the surrogate technique can be reliably utilized to determine (n,f) cross sections, where little or no data are available, it must first be shown to successfully reproduce known neutron-induced fission cross sections. The present experiment tests the surrogate technique, and specifically the so-called surrogate ratio method, when (p,d) and (p,t) surrogate reactions are employed to benchmark neutron-induced fission cross sections for uranium nuclei.

*rhughes2@richmond.edu

II. THEORETICAL BACKGROUND

The surrogate method assumes the Hauser-Feshbach formalism of CN formation and decay [13]. According to this formalism, the total cross section of a neutron-induced fission reaction is given by

$$\sigma_{(n,f)} = \sum_{J\pi} \sigma_n^{\mathrm{CN}}(E_n, J, \pi)\, G_f^{\mathrm{CN}}(E_n, J, \pi), \tag{1}$$

where σ_n^{CN} defines the cross section of CN formation in the neutron reaction and G_f^{CN} defines the probability that the CN will decay by fission. Both terms depend on the energy, spin, and parity of the CN. In the Weisskopf-Ewing limit [14] of Hauser-Feshbach theory, the fission decay probability, G_f^{CN}, depends only on the excitation energy (i.e., is assumed to be independent of the spin and parity).

If the desired neutron-induced reaction is written as A + n $\rightarrow$ C*, where C* is a compound nucleus state in statistical equilibrium [15–22], then the surrogate reaction to populate the same compound nucleus, C*, is given by B + b $\rightarrow$ C* + c. If CN formation is assumed to be independent of the entrance channel, the fission decay probability, $G_f^{\mathrm{CN}}(E_n)$, can be measured directly via the surrogate reaction according to

$$G_f^{\mathrm{CN}}(E_n) = \frac{N_{(b,cf)}}{\epsilon_f N_{(b,c)}}, \tag{2}$$

in which ϵ_f is the fission detection efficiency, $N_{(b,cf)}$, is the number of fission events detected in the surrogate reaction and $N_{(b,c)}$ is the total number of measured reactions (i.e., the total number of compound nuclei, C* produced). $N_{(b,c)}$ is given by

$$N_{(b,c)} = \sigma_c \epsilon_c \rho_T \ell_t Q, \tag{3}$$

where the terms represent reaction cross section (σ_c), particle detection efficiency (ϵ_c), areal target density (ρ_T),

experimental live time (ℓ_t), and integrated charge delivered by the particle beam (Q). If contaminants are present in a target, measuring $N_{(b,c)}$ can be difficult (if not impossible) and even small amounts of contamination lead to large errors in (n,f) cross sections determined via surrogate reactions (see, e.g., Ref. [5]). Once $G_f^{\rm CN}(E_n)$ is established, then $\sigma_n^{\rm CN}$ can be calculated with reasonable accuracy using an optical model, and the neutron-induced fission cross section deduced according to

$$\sigma_{(n,f)} = \sigma_n^{\rm CN} \frac{N_{(b,cf)}}{\epsilon_f N_{(b,c)}}. \tag{4}$$

The surrogate ratio method (SRM) [23,24] eliminates the requirement to measure $N_{(b,c)}$ and, thus, removes a large proportion of the systematic uncertainties inherent in surrogate measurements. In this case, two surrogate measurements with identical reactions and setup are performed for nuclei that can be assumed to have very similar structure (for example, neighboring, even-even isotopes). The ratio of Eq. (4) for the two experiments can then be taken, where the $N_{(b,c)}$ terms in the two experiments are assumed to cancel (i.e., CN formation cross sections in the surrogate reactions are the same). In specific cases, the CN formation cross sections for the two neutron-induced reactions, $\sigma_n^{\rm CN}$, also cancel. In other cases, $\sigma_n^{\rm CN}$ values can typically be calculated to good accuracy. The fission probability ratio of two surrogate experiments, X and Y, can subsequently be used to directly determine the ratio of two (n,f) cross sections according to

$$\frac{\sigma^X_{(n,f)}}{\sigma^Y_{(n,f)}} = C \frac{N^X_{(b,cf)}(E_n)}{N^Y_{(b,cf)}(E_n)}, \tag{5}$$

in which the normalization constant C is independent of energy and is given by

$$C = \frac{(\rho_T \ell_t Q)^Y}{(\rho_T \ell_t Q)^X}, \tag{6}$$

where the assumption has been made that the detection efficiencies (ϵ_c and ϵ_f) and reaction cross sections (σ_c) in the two surrogate experiments cancel.

In principle, two surrogate experiments can be chosen where one has a previously determined (n,f) cross section. The unknown cross section can then be extracted from the measured ratio. In the present work, cross-section ratios deduced in the (p,d) and (p,t) surrogate measurements are compared directly with well established (n,f) cross-section data for $^{233-236}$U, allowing the validity of the SRM in employing these reactions to be tested for the first time. Evaluated (n,f) cross-section data from the Evaluated Nuclear Data File (ENDF) VII/B library [25] are used for the comparisons in the current work. Other data evaluations such as the Evaluated Nuclear Data Library of Lawrence Livermore National Laboratory (LLNL), ENDL-2009 [26], and the Japanese Evaluated Nuclear Data Library, JENDL-3.3 [27], show very similar (n,f) cross-section data over the energy ranges of interest.

III. EXPERIMENTAL PROCEDURE

A 28-MeV proton beam from the 88-Inch Cyclotron at Lawrence Berkeley National Laboratory was used to bombard ^{236}U and ^{238}U targets. The ^{236}U target was prepared by electrodepositing isotopically enriched material on a 100-μg/cm^2 carbon foil and was measured to have an areal density of 322(18) μg/cm^2 by α counting. The ^{238}U target was a self-supporting metallic 1450(90)-μg/cm^2-thick foil. For both targets, contaminant actinide species were less than 1%.

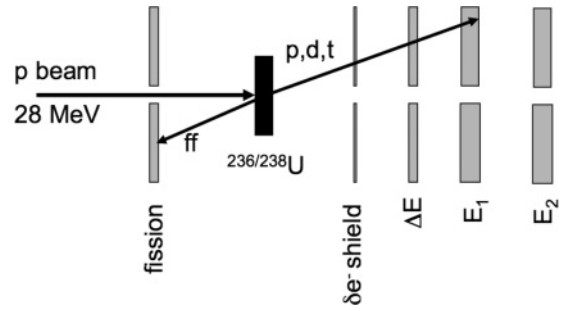

FIG. 1. Schematic diagram of the STARS array at Lawrence Berkeley National Laboratory.

The Silicon Telescope Array for Reaction Studies (STARS), shown schematically in Fig. 1, was used to measure outgoing deuterons and tritons over an angular range of 34°–64°. For this experiment STARS consisted of one 140 μm (ΔE) and two 1000 μm ($E1$ and $E2$) Micron $S2$ type silicon detectors. Coincident fission fragments were measured at backward angles between 109° and 137° using a second 140-μm Micron $S2$ type detector. Each $S2$ detector is segmented into 48 rings on one side and 16 sectors on the other. For the present experiment the rings and sectors were bussed together so each detector had 8 sectors and 24 one-millimeter rings to measure incident charged particles. The target position was placed 16 mm from the front face of the ΔE detector. A 4-mg/cm^2 Al δ-electron shield was placed between the target and the ΔE detector. This shield was sufficiently thick to stop forward-going fission fragments as well as δ electrons produced in the target. The STARS chamber was surrounded by six clover γ-ray detectors from the Livermore-Berkeley Array for Collaborative Experiments (LIBERACE), allowing for both particle-fission and particle-γ coincidence events to be collected.

Valid particle events required a light ion to be detected in both the ΔE and $E1$ detectors ($E2$ events were collected passively, although the triton and deuteron energy ranges studied in the present work meant that all particles were stopped in the $E1$ detector). A particle-fission time-to-amplitude converter (TAC) was utilized to isolate prompt particle-fission coincidences, and particles were tracked using the ring and sector information in the ΔE and $E1$ detectors so only single-particle events originating from the target position were selected. A particle-γ TAC was also used for isolating prompt particle-γ coincidence data.

Particle-singles, particle-γ, and particle-fission coincidence data were collected for 24.96 h on the ^{236}U target with an average proton beam intensity of 1.04(2) enA and an average 90.7(2)% live time. For the ^{238}U target, the integrated beam time was 69.8 h with an average intensity of 0.70(2) enA and an average live time of 88.1(2)%.

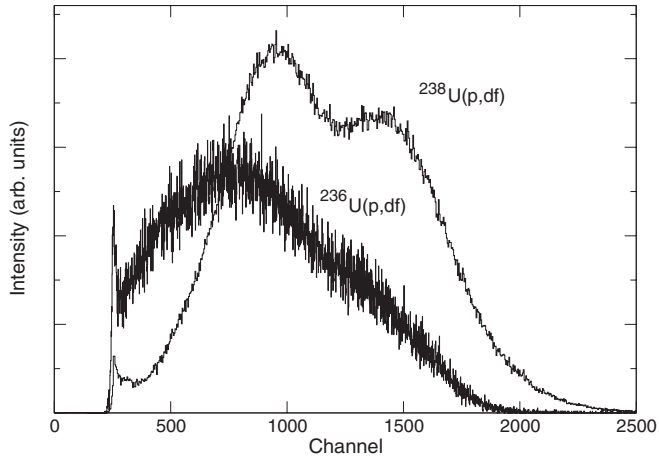

FIG. 2. Fission spectrum obtained in coincidence with deuterons measured in the ^{236}U$(p,d)^{235}$U and ^{238}U$(p,d)^{237}$U reactions. The fission spectrum associated with the ^{236}U target is broader and pushed to lower energy.

Spectra showing the fission events in coincidence with deuterons in the ^{236}U$(p,df)^{235}$U and ^{238}U$(p,df)^{237}$U reactions are shown in Fig. 2. (The fission spectra associated with tritons look similar to those for deuterons in both targets.) The spectrum seen for ^{238}U shows peaks associated with the low- and high-mass fission fragments. For the ^{236}U target, the fission spectrum is broader and pushed down in energy so it is cut off at the low energy range. (Note that the ^{236}U target data statistics are also much lower.) The distortion of the fission spectrum could be a result of significant carbon and oxygen contamination in the ^{236}U target (from the electroplating process), leading to increased energy straggling of the outgoing fission fragments.

To convert the measured charged particle energies into equivalent neutron energies, E_n, they must, first, be converted into CN excitation energies. This is achieved by correcting for the recoil energy imparted to the CN, the energy loss of the charged particle in the target, δ-electron shield and detector dead layers, and the reaction Q value. The energy scale is then set to be at $E_n = 0$ MeV coinciding with the CN neutron separation energy, S_n for each surrogate reaction.

A. Normalization factor and uncertainties

For the present experiment, the normalization factor given by Eq. (6) is calculated to be $C = 8.23(74)$. This value must be corrected to account for the fission fragments cut off at low energies for the ^{236}U target (see Fig. 2). It is estimated that 8.4% of the ^{236}U target fission spectrum is missing on the low energy end and the final normalization used in the present work is therefore corrected to $C = 8.92(80)$. The systematic error of 9% includes uncertainties from the live time and integrated beam on target measured in the two experiments but is dominated by the target thickness uncertainties.

The energy uncertainty in the present work is determined to be about 100 keV from the 1σ width associated with Gaussian fits of discrete population peaks in the particle spectra associated with ^{235}U, ^{236}U, and ^{237}U (deduced from the particle-γ coincidence data) as summarized in Table I. The factors leading to this value can be ascribed to energy straggle of outgoing light ions in the target and detection system, angular detection resolution, intrinsic detector resolution, and cyclotron beam energy resolution.

TABLE I. Energy uncertainties deduced from the 1σ widths of discrete direct population peaks of levels in various uranium isotopes. The discrete peaks are isolated from the particle-γ coincidence data by gating on specific γ-ray energies. The adopted energy uncertainty is the mean of the widths measured in the different data sets. Note there were insufficient particle-γ statistics to measure discrete level widths associated with the ^{236}U$(p,t)^{234}$U reaction.

Reaction	Level/γ-ray energy (keV)	1σ peak width (keV)
^{236}U$(p,d)^{235}$U	659/646	102
^{238}U$(p,t)^{236}$U	958/958	94
^{238}U$(p,d)^{237}$U	864/852	98
Adopted energy uncertainty		98

The distribution of fission fragments with respect to the recoiling nucleus is anisotropic [28] and can also potentially introduce an energy-dependent uncertainty to the present results. To test whether this affects the (p,df) and (p,tf) studies, a similar approach to Ressler *et al.* [12] is applied. The ratio of fission fragments measured in-plane and out of the plane of the outgoing light ions is deduced for both (p,d) and (p,t) reactions as a function of equivalent neutron energy. In-plane fission events are defined as occurring in the same or opposite sector elements of the fission detector as the associated light ions in the ΔE detector. Out-of-plane fission events are defined to be those that occur in the two orthogonal sector elements of the fission detector with respect to light ions measured in the ΔE detector. As shown in Fig. 3, it is

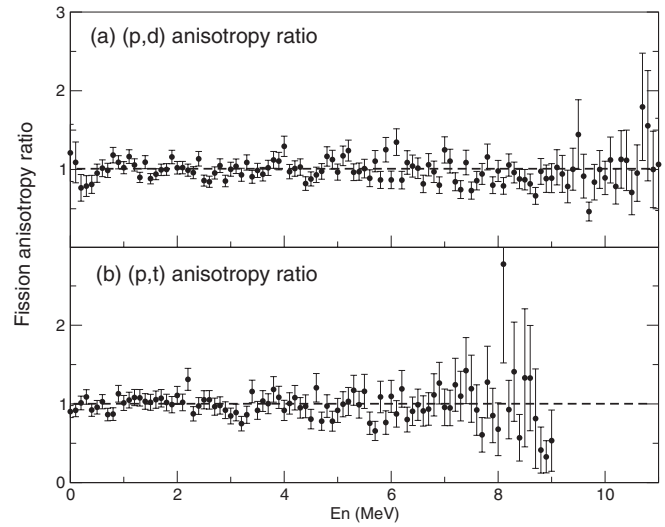

FIG. 3. Fission fragment anisotropy ratios as a function of equivalent neutron energy (as defined in the text). (a) The ^{236}U$(p,df)^{235}$U/^{238}U$(p,df)^{237}$U anisotropy ratio. (b) The ^{236}U$(p,tf)^{234}$U/^{238}U$(p,tf)^{236}$U anisotropy ratio. The values scatter around unity suggesting fission anisotropies approximately cancel and should not affect the surrogate measurements.

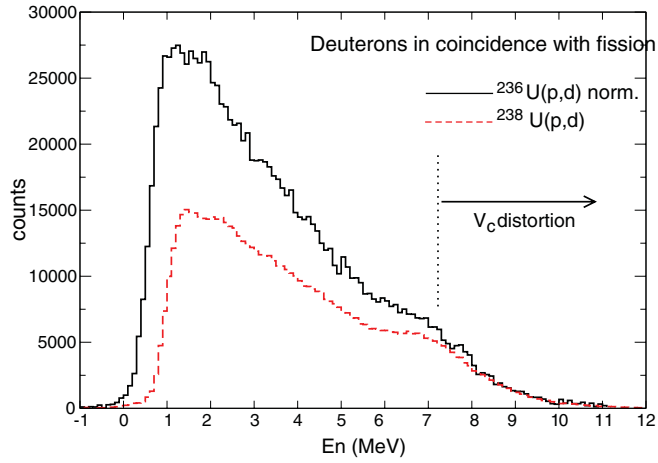

FIG. 4. (Color online) Comparison of deuteron spectra for the ^{238}U$(p,df)^{237}$U and ^{236}U$(p,df)^{235}$U reactions. The ^{236}U$(p,df)^{235}$U data have been normalized to correct for the different integrated beam and target thicknesses in the two experiments. The region beyond ~7 MeV is distorted as described in the text.

observed that the relative anisotropies for the (p,d) and (p,t) reactions on the two targets is approximately unity and is, thus, neglected in the present work.

IV. RESULTS

A. The ^{238}U$(p,df)^{237}$U/^{236}U$(p,df)^{235}$U surrogate measurement

The particle spectra for ^{238}U$(p,df)^{237}$U (dotted line) and ^{236}U$(p,df)^{235}$U (solid line) are presented in Fig. 4. The ^{236}U(p,df) spectrum has been normalized to the ^{238}U(p,df) data according to Eq. (6), and both spectra are compressed to 100 keV/chan. The neutron separation energies for ^{235}U and ^{237}U are 5.19 and 5.13 MeV, respectively [29]. The spectra in Fig. 4 are adjusted so the equivalent neutron energies, E_n, are zero at these energies. There is a rapid falloff in the number of deuterons beyond about $E_n \sim 7$ MeV (and above) in both spectra. This energy corresponds to deuteron energies of ~12 MeV (and below), i.e., deuterons with energies lower than the Coulomb barrier, V_c, for the deuteron-CN system. The desired cross-section ratio is extracted from the ratio of the particle spectra in Fig. 4 and using Eq. (5).

Figure 5(a) presents the $\sigma[^{236}\mathrm{U}(n,f)]/\sigma[^{234}\mathrm{U}(n,f)]$ cross-section ratio deduced from the ^{238}U$(p,df)/^{236}$U(p,df) surrogate data (points with error bars). The ratio from the ENDF/B-VII values (solid line) is also shown. Figure 5(b) compares the extracted $\sigma[^{236}\mathrm{U}(n,f)]$ cross section (points with error bars) to the ENDF/B-VII values (solid line). The data show good agreement with the ENDF/B-VII values (within ~7%) to $E_n \sim 7$ MeV, albeit the surrogate ratio in Fig. 5(a) is consistently higher than that in the ENDF/B-VII data. Angular-momentum transfer differences between the surrogate and neutron-induced reactions are typically expected to cause deviations at low energies ($E_n < 1$ MeV), as well as at the onset of second-chance fission [24]. Figure 5(a) may show some indication of the effect, but there is little impact on the extracted cross section. Beyond $E_n \sim 7$ MeV, there is a rapid deviation of the surrogate measurement from the directly measured cross-section ratio. This is likely to be associated with the rapid falloff in particle statistics due to the Coulomb barrier effects discussed above, being magnified by the relative energy scale shifts in the two surrogate experiments (due to slightly different Q values and S_n values).

B. The ^{238}U$(p,tf)^{236}$U/ ^{236}U$(p,tf)^{234}$U surrogate measurement

The particle spectra for ^{238}U$(p,tf)^{236}$U (dotted line) and ^{236}U$(p,tf)^{234}$U (solid line) are presented in Fig. 6. The ^{236}U(p,tf) spectrum has again been normalized to the ^{238}U(p,tf) data according to Eq. (6). Both spectra are once more compressed to 100 keV/chan. The neutron separation

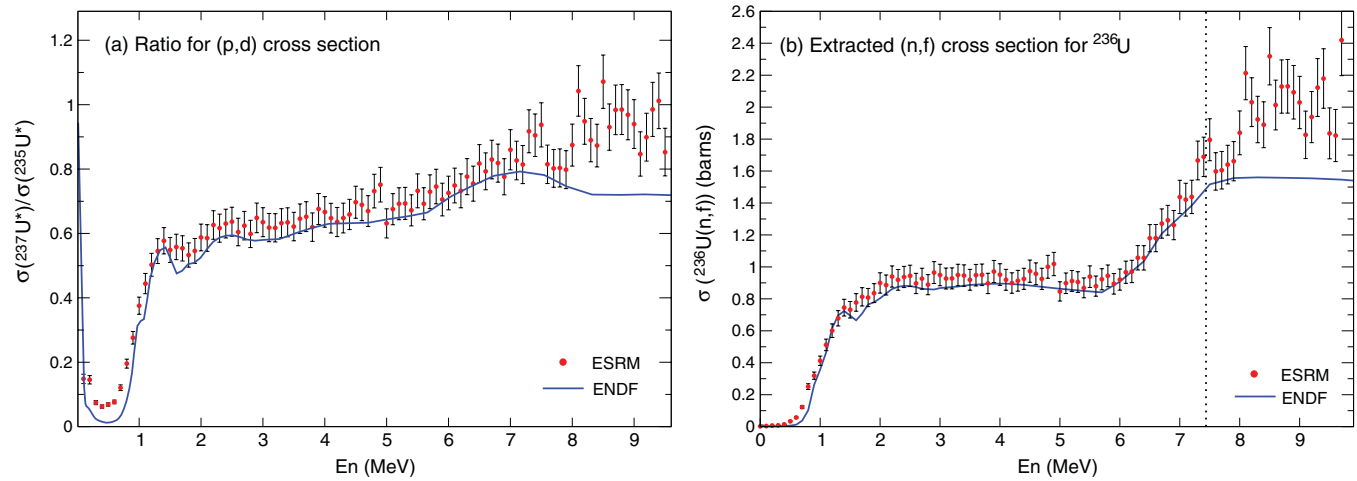

FIG. 5. (Color online) (a) The $\sigma[^{236}\mathrm{U}(n,f)]/\sigma[^{234}\mathrm{U}(n,f)]$ ratio determined from the ^{238}U$(p,df)^{237}$U and ^{236}U$(p,df)^{235}$U surrogate measurements (data points) and compared to the ENDF/B-VII value for the ratio (solid line). (b) The $\sigma[^{236}\mathrm{U}(n,f)]$ cross section extracted from the surrogate ratio in (a) and the ENDF/B-VII $\sigma[^{234}\mathrm{U}(n,f)]$ cross section (data points) being compared to the ENDF/B-VII $\sigma[^{236}\mathrm{U}\,(n,f)]$ cross section (solid line). The vertical dotted line represents the approximate energy beyond which the extracted cross section becomes unreliable. Energy uncertainties of 98 keV are omitted from the data points for clarity.

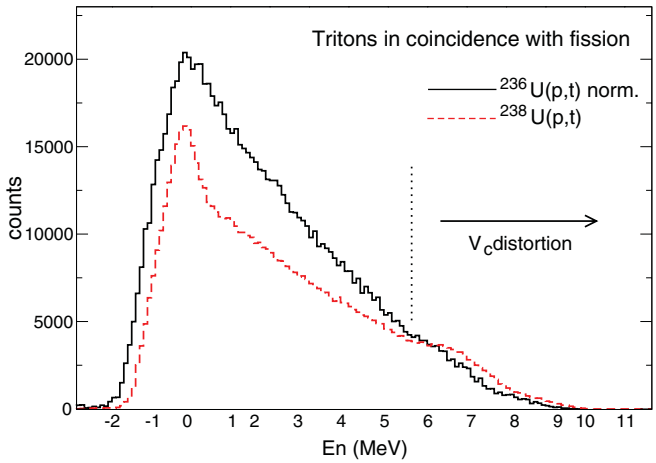

FIG. 6. (Color online) Comparison of triton spectra for the ^{238}U$(p,tf)^{236}$U and ^{236}U$(p,tf)^{234}$U reactions. The ^{236}U$(p,tf)^{234}$U data have been normalized to correct for the different integrated beam and target thicknesses in the two experiments. Similarly to the above (p,df) data the region beyond ~5.5 MeV is distorted.

energies for ^{234}U and ^{236}U are 6.8 MeV [30] and 6.5 MeV [31], respectively. The energy spectra in Fig. 6 are adjusted so the equivalent neutron energy, E_n is zero at these respective energies.

The $\sigma[^{235}\mathrm{U}(n,f)]/\sigma[^{233}\mathrm{U}(n,f)]$ cross-section ratio deduced from the ^{238}U$(p,tf)/^{236}$U(p,tf) surrogate data (points with error bars) is compared to the ratio from the ENDF/B-VII values (solid line) in Fig. 7(a). Figure 7(b) compares the extracted $\sigma[^{235}\mathrm{U}(n,f)]$ cross section (points with error bars) to the ENDF/B-VII values (solid line). There is good agreement (within ~6%) up to about 5.5 MeV, where the outgoing triton energies fall below the $V_c \approx 12$-MeV Coulomb barrier. The good agreement seen at low energy ($E_n < 1$ MeV) implies that angular-momentum transfer differences between the surrogate and neutron-induced reactions do not play a major role [24]. The triton surrogate ratio deviates from the ENDF/B-VII ratio at an apparent lower equivalent neutron energy than the deuteron surrogate ratio ($E_n \sim 7$ MeV) partially due to the higher S_n value for the ^{234}U and ^{236}U compound systems relative to ^{235}U and ^{237}U. Similarly to the (p,d) data, the surrogate ratio lies slightly higher than the ENDF/B-VII ratio on average (albeit within error).

C. The $(p,d)/(p,t)$ internal surrogate ratio measurement

The present results rely on the assumption that CN formation is independent of the entrance channel. The good agreement seen for the extracted cross-section ratios discussed above suggest that this assumption is fairly robust for (p,d) and (p,t) reactions. In principle, it is also possible to perform a surrogate ratio measurement on a single target from the measured fission cross sections associated with two reaction channels. Such a ratio method was recently employed by Nayak *et al.* [6] to determine the ^{233}Pa(n,f) cross section by utilizing $(^6\mathrm{Li},\alpha)$ and $(^6\mathrm{Li},d)$ surrogate reactions. In the ^{233}Pa(n,f) case, the absence of previous experimental data in the $E_n = 11.5$–16.5 MeV energy range meant that the extracted data points could not be compared to direct (n,f) measurements.

In the present work, the $(p,df)/(p,tf)$ cross-section ratio can be measured internally for both the ^{236}U and ^{238}U targets and the results compared to the equivalent (n,f) cross-section ratios from the ENDF/B-VII evaluation. In contrast to the external SRM discussed above, this technique removes the requirement of correcting target data sets relative to one another [using Eqs. (5) and (6)], since both sets of data are collected simultaneously from the same target. However, the data from two reaction channels must be normalized to account for different absolute reaction cross sections, σ_c, associated with the different exit channels. Furthermore, it must be

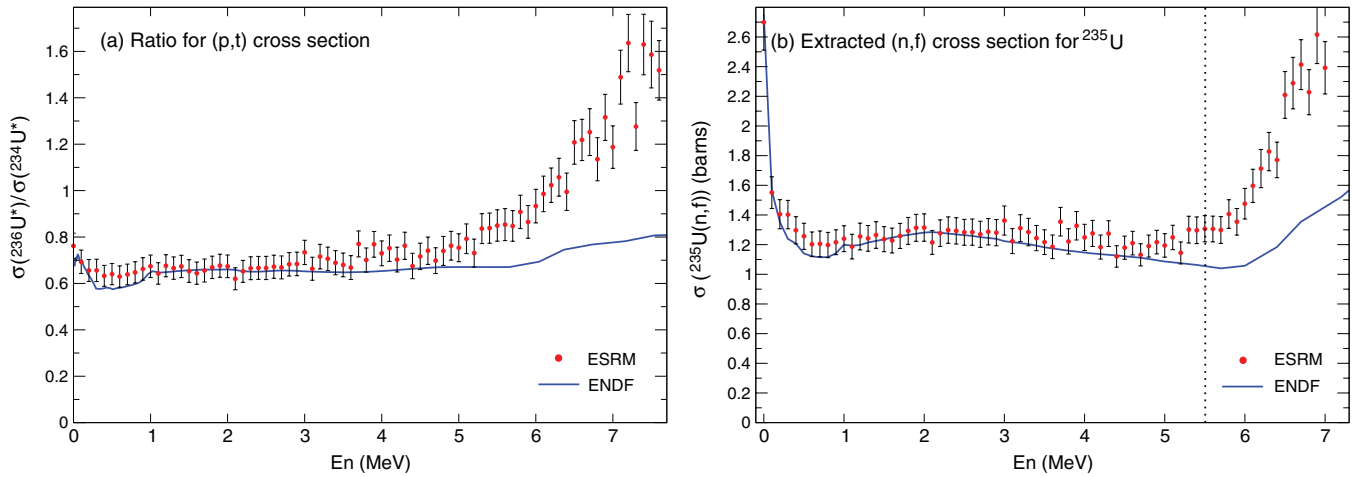

FIG. 7. (Color online) (a) The $\sigma[^{235}\mathrm{U}(n,f)]/\sigma[^{233}\mathrm{U}(n,f)]$ ratio as determined from the ^{238}U$(p,tf)^{236}$U and ^{236}U$(p,tf)^{234}$U surrogate measurements (data points) and compared to the ENDF/B-VII value for the ratio (solid line). (b) The $\sigma[^{235}\mathrm{U}(n,f)]$ cross section extracted from the ratio in (a) and the ENDF/B-VII $\sigma[^{233}\mathrm{U}(n,f)]$ cross section (data points) is compared to the ENDF/B-VII $\sigma[^{235}\mathrm{U}(n,f)]$ cross section (solid line). The vertical dotted line represents the approximate energy beyond which the extracted cross section becomes unreliable. Energy uncertainties of 98 keV are omitted from the data points for clarity.

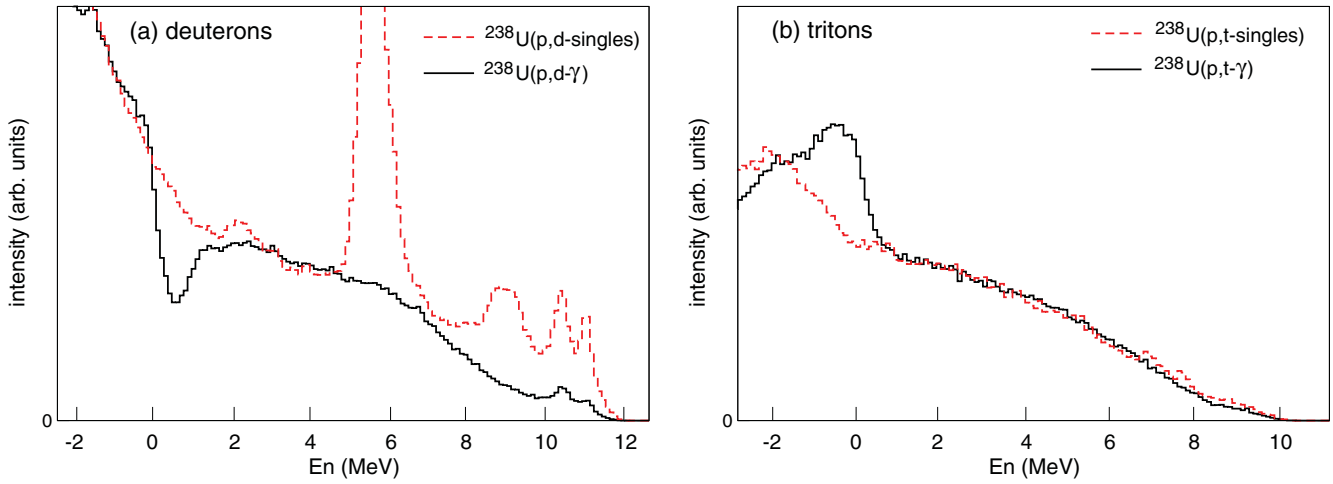

FIG. 8. (Color online) Comparison of particle-singles spectra and particle-γ spectra (with a prompt particle-γ TAC gate) for deuterons and tritons. The particle-singles and particle-γ data have been normalized relative to one another. (a) Deuterons: The d-γ spectrum shows a dip where the neutron emission and fission channels open up ($E_n = 0$–1 MeV). Light ion contaminant lines are apparent between 2 and 12 MeV in the singles spectrum. (b) Tritons: The γ rays associated with fission make a bump in the spectrum up to $E_n \sim 0.5$ MeV (this is due to the fission channel opening up below S_n). Few contaminant peaks are apparent in the triton singles spectrum. For both deuterons and tritons, the particle-γ spectra are smooth between $E_n = 1$–5 MeV.

assumed that the deuteron and triton detection efficiencies are comparable across the appropriate energy ranges. If X and Y are surrogate measurements using the (p,d) and (p,t) respective reaction channels, then the neutron-induced fission cross-section ratio, deduced from Eqs. (2), (3), and (4), is given by

$$\frac{\sigma^X_{(n,f)}}{\sigma^Y_{(n,f)}} = \frac{N^X_{(p,df)}(E_n)}{N^X_{(p,d)}(E_n)} \Big/ \frac{N^Y_{(p,tf)}(E_n)}{N^Y_{(p,t)}(E_n)} = \frac{\sigma^Y_{(p,t)} N^X_{(p,df)}(E_n)}{\sigma^X_{(p,d)} N^Y_{(p,tf)}(E_n)}. \tag{7}$$

Ideally, the absolute reaction cross-section ratio, $\sigma^Y_{(p,t)}/\sigma^X_{(p,d)}$, would be extracted over the equivalent neutron energy ranges of interest from particle-singles data. However, this carries the drawback inherent to the absolute surrogate method eluded to earlier; namely target contaminants can introduce large systematic errors or even completely distort measurements that utilize particle-singles data. In the present work, the ratio, $\sigma^Y_{(p,t)}/\sigma^X_{(p,d)}$, was extracted from particle-γ coincidence data, using particles in coincidence with any γ ray and utilizing a prompt particle-γ TAC gate to eliminate contaminants [note that particle-γ events associated with (p,d) and (p,t) reactions on light ion contaminant species are negligible within the energy ranges of interest].

For the particle-γ data to give an accurate cross-section correction, the deuteron and triton spectra observed in coincidence with γ rays must be proportional to the singles deuteron and triton spectra. This is equivalent to the statement that each CN produced in coincidence with a deuteron or a triton also emits γ rays in prompt coincidence with its decay. The two dominant modes of CN decay between $E_n = 1$–5 MeV are fission and neutron emission. The fission decay channel will result in γ-ray decays from the fission fragments. Gamma decay also accompanies neutron emission, unless it directly populates the ground state of the daughter nucleus. Given the low γ-ray detection efficiencies (typically 1–3%) in the present work, different γ-ray multiplicities associated with the fission and neutron-emission decay channels may affect the correlation between the particle-singles and particle-γ data.

A comparison of the particle-singles and particle-γ spectra for the ^{238}U target data is shown for both (p,d) and (p,t) reactions in Fig. 8. The deuteron-singles spectrum (dotted line) in Fig. 8(a) exhibits several contaminant peaks between $E_n = 2$–12 MeV. For example, the largest peaks at about 5.8 and 9 MeV represent direct ground-state population in the ^{16}O$(p,d)^{15}$O and ^{12}C$(p,d)^{11}$C reactions, respectively. These contaminant lines would result in an unreliable cross-section correction if it were extracted from the singles data. In the corresponding particle-γ data (solid line), all contaminant lines except for those between $E_n = 10$–12 MeV are eliminated when requiring a coincident γ ray. The particle-γ spectrum associated with deuterons is, therefore, clear of contaminants in the energy region of interest between $E_n = 1$–5 MeV. In contrast to the deuteron data, almost no contaminant peaks are observed in the triton-singles spectrum (dotted line) in Fig. 8(b). For the triton-γ spectrum (solid line), the data trend proportionally to the singles data above $E_n = 1$ MeV, giving some confidence in the assumed correlation between the particle-singles and particle-γ data. The ^{236}U target data also show smoothly trending deuteron-γ and triton-γ spectra between about $E_n = 1$–5 MeV (albeit with lower statistics).

Due to low particle-γ statistics associated with the ^{236}U target data, and the observed nonuniformity of the particle-γ data below $E_n \sim 1$ MeV for both target data sets (see Fig. 8), the $\sigma^Y_{(p,t)}/\sigma^X_{(p,d)}$ ratio is taken to be constant as a function of outgoing particle energy. The value was obtained for both target data sets from the ratio of the total number of tritons and deuterons observed in coincidence with γ rays, between $E_n = 1$–5 MeV. For the ^{236}U target, a relative cross-section correction of $\sigma[^{236}\text{U}(p,d)^{235}\text{U}/^{236}\text{U}(p,t)^{234}\text{U}] = 2.34(17)$ was determined, while for the ^{238}U target, a value of $\sigma[^{238}\text{U}(p,d)^{237}\text{U}/^{238}\text{U}(p,t)^{236}\text{U}] = 2.55(15)$ was obtained.

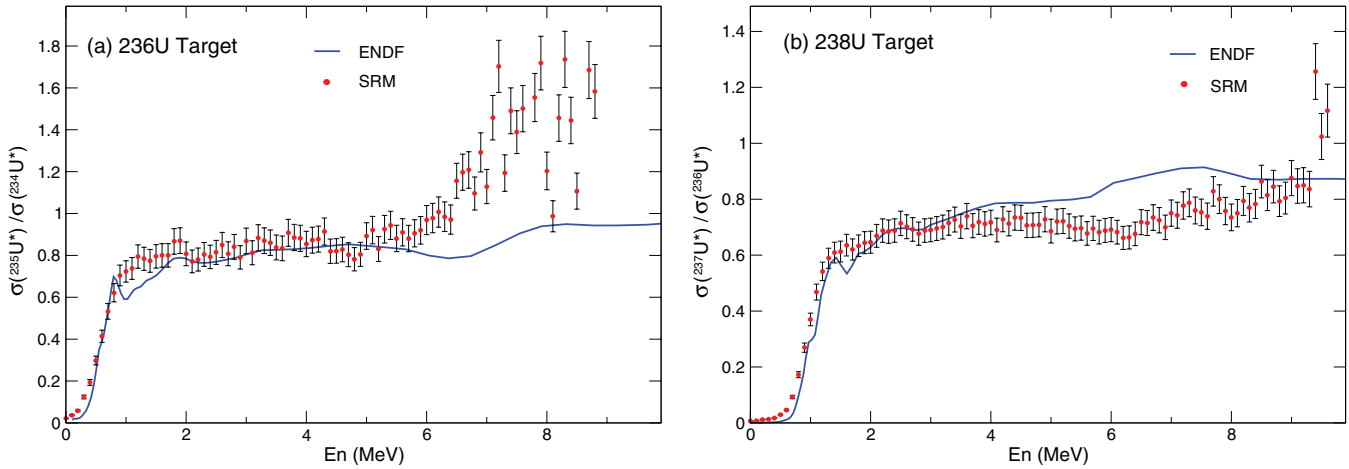

FIG. 9. (Color online) (a) The $\sigma[^{234}\mathrm{U}(n,f)]/\sigma[^{233}\mathrm{U}(n,f)]$ ratio from the $^{236}\mathrm{U}(p,d)^{235}\mathrm{U}/^{236}\mathrm{U}(p,t)^{234}\mathrm{U}$ surrogate ratio (data points) compared to the ENDF/B-VII ratio (solid line). (b) The $\sigma[^{236}\mathrm{U}(n,f)]/\sigma[^{235}\mathrm{U}(n,f)]$ ratio from the $^{238}\mathrm{U}(p,d)^{237}\mathrm{U}/^{238}\mathrm{U}(p,t)^{236}\mathrm{U}$ surrogate ratio (data points) compared to the ENDF/B-VII ratio (solid line). Energy uncertainties of 98 keV are omitted from the data points for clarity.

These values were used to correct each data point in the (p,tf) spectra relative to the (p,df) spectra (shown in Figs. 4 and 6) for both the $^{236}\mathrm{U}$ and $^{238}\mathrm{U}$ target data. The resulting surrogate ratios for both targets are compared to the ENDF/B-VII ratios in Fig. 9.

For both targets, the $(p,df)/(p,tf)$ surrogate ratios compare remarkably well (within ∼15%) to the ENDF/B-VII (n,f) cross-section ratios up to ∼5 MeV. This is the approximate energy where the (p,tf) external surrogate ratio discussed in the previous section deviated from the (n,f) data and is, again, possibly an upper limit determined by the effect of the Coulomb barrier on low-energy deuterons/tritons.

The extracted ratio for both targets is very sensitive to the relative $\sigma^{Y}_{(p,t)}/\sigma^{X}_{(p,d)}$ cross-section correction. The energy range over which the correction is selected can significantly alter the extracted ratio, specifically when energies below $E_n = 1$ MeV are included. Ideally, the relative cross-section correction would include an energy dependence to take into account possible changes in the relative cross section with energy.

V. SUMMARY

In summary, neutron-induced fission cross-section ratios of various uranium isotopes have been indirectly determined via the surrogate ratio method. The $\sigma[^{236}\mathrm{U}(n,f)]/\sigma[^{234}\mathrm{U}(n,f)]$ cross-section ratio was measured via (p,d) reactions on $^{238}\mathrm{U}$ and $^{236}\mathrm{U}$ targets and the $\sigma[^{235}\mathrm{U}(n,f)]/\sigma[^{233}\mathrm{U}(n,f)]$ cross-section ratio was determined via (p,t) reactions on the same targets. The extracted cross-section ratios for (p,d) and (p,t) surrogate reactions compare well to accepted $\sigma(n,f)$ ratios in the approximate equivalent neutron energy ranges $E_n = 0$–7 MeV and $E_n = 0$–5.5 MeV, respectively. In both cases the upper limit on the reliable cross-section energy extraction is restricted by the outgoing light ion energies falling below the Coulomb barrier at slightly different equivalent neutron energies in the two surrogate experiments. The energy range could be extended by the use of a higher beam energy to overcome the Coulomb barrier effects, however, careful selection of appropriate detector thicknesses and geometry (relative to the target) is necessary to ensure outgoing deuterons and tritons are stopped within the detection system.

An internal surrogate ratio measurement comparing the (p,df) and (p,tf) reaction channels on $^{236}\mathrm{U}$ and separately on $^{238}\mathrm{U}$ has also been investigated. This technique avoids the necessity of two separate experiments, as well as a relative normalization to account for different integrated beam and target thicknesses. However, the internal method necessitates a relative correction to account for the different reaction channel cross sections [in this case $\sigma(p,d)$ and $\sigma(p,t)$]. Such a correction can be difficult to extract from particle singles data due to target contamination. In the present work, the correction was deduced from the particle-γ coincidence data where a particle-γ TAC was utilized to remove most target contaminant artifacts. For both the $^{236}\mathrm{U}$ and $^{238}\mathrm{U}$ targets, the (n,f) cross-section ratios deduced from the $(p,df)/(p,tf)$ data agree to within about 15% of the accepted values in the equivalent neutron energy range $E_n = 0$–5 MeV. The surrogate ratio method, therefore, seems to extend to ratios using different reaction channels with the same target. However, more work is needed to test the efficacy of using particle-γ coincidence data to extract a reliable, energy-dependent cross-section correction. It is also worth extending investigations of internal surrogate ratio measurements to the use of different reactions, such as $(\alpha,{}^3\mathrm{He})/(\alpha,\alpha')$ and $(d,p)/(d,t)$ surrogate ratios.

ACKNOWLEDGMENTS

The authors thank the 88-Inch Cyclotron operations and facilities staff. We also thank the Department of Energy's NNSA, Office of Non-Proliferation Research and Development (NA-22), for financial support. This work was supported by the U. S. Department of Energy under Grants No. DE-FG02-05 ER41379 and No. DE-FG52-06 NA26206 (University of Richmond), No. DE- AC52-07NA27344 (Lawrence Livermore National Laboratory), and No. DE-AC02-05CH11231 (Lawrence Berkeley National Laboratory).

[1] J. D. Cramer and H. C. Britt, Nucl. Sci. Eng. **41**, 177 (1970).
[2] J. D. Cramer and H. C. Britt, Phys. Rev. C **2**, 2350 (1970).
[3] M. Petit, M. Aiche, G. Barreau, S. Boyer, N. Carjan, S. Czajkowski, D. Dassié, C. Grosjean, A. Guiral, B. Haas, D. Karamanis, S. Misicu, 4, C. Rizea, F. Saintamon, S. Andriamonje, E. Bouchez, F. Gunsing, A. Hurstel, Y. Lecoz, R. Lucas, Ch. Theisen, A. Billebaud, L. Perrot, and E. Bauge, Nucl. Phys. A **735**, 345 (2004).
[4] J. T. Harke, L. A. Bernstein, J. Escher, L. Ahle, J. A. Church, F. S. Dietrich, K. J. Moody, and E. B. Norman, Phys. Rev. C **73**, 054604 (2006).
[5] B. F. Lyles, L. A. Bernstein, J. T. Harke, F. S. Dietrich, J. Escher, and I. Thompson, Phys. Rev. C **76**, 014606 (2007).
[6] B. K. Nayak, A. Saxena, D. C. Biswas, E. T. Mirgule, B. V. John, S. Santra, R. P. Vind, R. K. Choudhury, and S. Ganesan, Phys. Rev. C **78**, 061602(R) (2008).
[7] S. R. Lesher, J. T. Harke, L. A. Bernstein, H. Ai, C. W. Beausang, D. L. Bleuel, R. M. Clark, F. S. Dietrich, J. E. Escher, P. Fallon, J. Gibelin, B. L. Goldblum, I. Y. Lee, A. O. Macchiavelli, M. A. McMahan, K. J. Moody, E. B. Norman, L. Phair, E. Rodriguez-Vieitez, N. D. Scielzo, and M. Wiedeking, Phys. Rev. C **79**, 044609 (2009).
[8] M. S. Basunia, R. M. Clark, B. L. Goldblum, L. A. Bernstein, L. Phair, J. T. Burke, C. W. Beausang, D. L. Bleuel, B. Darakchieva, F. S. Dietrich, M. Evtimova, P. Fallon, J. Gibelin, R. Hatarik, C. C. Jewett, S. R. Lesher, M. A. McMahan, E. Rodriguez-Vieitez, and M. Wiedeking, Nucl. Instrum. Methods Phys. B **267**, 1899 (2009).
[9] J. M. Allmond, L. A. Bernstein, C. W. Beausang, L. Phair, D. L. Bleuel, J. T. Harke, J. E. Escher, K. E. Evans, B. L. Goldblum, R. Hatarik, H. B. Jeppesen, S. R. Lesher, M. A. McMahan, J. O. Rasmussen, N. D. Scielzo, and M. Wiedeking, Phys. Rev. C **79**, 054610 (2009).
[10] B. L. Goldblum, S. R. Stroberg, J. M. Allmond, C. Angell, L. A. Bernstein, D. L. Bleuel, J. T. Harke, J. Gibelin, L. Phair, N. D. Scielzo, E. Swanberg, M. Wiedeking, and E. B. Norman, Phys. Rev. C **80**, 044610 (2009).
[11] G. Kessedjian, B. Jurado, M. Aiche, G. Barreau, A. Bidaud, S. Czajkowski, D. Dassié, B. Haas, L. Mathieu, L. Audouin, N. Capellan, L. Tassan-Got, J. N. Wilson, E. Berthoumieux, F. Gunsing, Ch. Theisen, O. Serot, E. Bauge, I. Ahmad, J. P. Greene, and R. V. F. Janssens, Phys. Lett. B **692**, 297 (2010).
[12] J. J. Ressler, J. T. Harke, J. E. Escher, C. T. Angell, M. S. Basunia, C. W. Beausang, L. A. Bernstein, D. L. Bleuel, R. J. Casperson, B. L. Goldblum, J. Gostic, R. Hatarik, R. Henderson, R. O. Hughes, J. Munson, L. W. Phair, T. J. Ross, N. D. Scielzo, E. Swanberg, I. J. Thompson, and M. Wiedeking, Phys. Rev. C **83**, 054610 (2011).
[13] W. Hauser and H. Feshbach, Phys. Rev. **87**, 366 (1952).
[14] V. F. Weisskopf and D. H. Ewing, Phys. Rev. **57**, 472 (1940).
[15] J. Escher, L. Ahle, L. Bernstein, J. A. Church, F. Dietrich, C. Forssén, and R. Hoffman, Nucl. Phys. A **758**, 86c (2005).
[16] J. Escher, L. Ahle, L. Bernstein, J. Burke, J. A. Church, F. Dietrich, C. Forssén, V. Gueorguiev, and R. Hoffman, J. Phys. G **31**, S1687 (2005).
[17] C. Forssén, L. Ahlea, L. A. Bernsteina, J. A. Churcha, F. S. Dietrichа, J. Eschera, and R. D. Hoffman, Nucl. Phys. A **758**, 130c (2005).
[18] J. A. Church, L. Ahle, L. A. Bernstein, J. Cooper, F. S. Dietrich, J. Escher, C. Forssen, H. Ai, H. Amro, M. Babilon, C. Beausang, J. Caggiano, A. Heinz, R. Hughes, E. McCutchan, D. Meyer, C. Plettner, J. Ressler, and V. Zamfir, Nucl. Phys. A **758**, 126c (2005).
[19] W. Younes and H. C. Britt, Phys. Rev. C **67**, 024610 (2003).
[20] W. Younes and H. C. Britt, Phys. Rev. C **68**, 034610 (2003).
[21] W. Younes, H. C. Britt, J. A. Becker, and J. B. Wilhelmy, LLNL Tech. Rep. No. UCRL-ID-154194, 2003 (unpublished).
[22] H. C. Britt and J. B. Wilhelmy, Nucl. Sci. Eng. **72**, 222 (1979).
[23] C. Plettner, H. Ai, C. W. Beausang, L. A. Bernstein, L. Ahle, H. Amro, M. Babilon, J. T. Harke, J. A. Caggiano, R. F. Casten, J. A. Church, J. R. Cooper, B. Crider, G. Gürdal, A. Heinz, E. A. McCutchan, K. Moody, J. A. Punyon, J. Qian, J. J. Ressler, A. Schiller, E. Williams, and W. Younes, Phys. Rev. C **71**, 051602(R) (2005).
[24] J. E. Escher and F. S. Dietrich, Phys. Rev. C **74**, 054601 (2006).
[25] M. B. Chadwick, P. Obložinský, M. Herman, N. M. Greene, R. D. McKnight, D. L. Smith, P. G. Young, R. E. MacFarlane, G.M. Hale, S. C. Frankle, A. C. Kahler, T. Kawano, R. C. Little, D. G. Madland, P. Moller, R. D. Mosteller, P. R. Page, P. Talou, H. Trellue, M. C. White, W. B. Wilson, R. Arcilla, C. L. Dunford, S. F. Mughabghab, B. Pritychenko, D. Rochman, A. A. Sonzogni, C. R. Lubitz, T. H. Trumbul, J. P. Weinman, D. A. Brown, D. E. Cullen, D. P. Heinrichs, D. P. McNabb, H. Derrien, M. E. Dunn, N. M. Larson, L. C. Leal, A. D. Carlson, R. C. Block, J. B. Briggs, E. T. Cheng, H. C. Huria, M. L. Zerkle, K. S. Kozier, A. Courcelle, V. Pronyaev, and S. C. van der Marck, Nucl. Data Sheets **107**, 2931 (2006).
[26] B. Beck *et al.*, LLNL-TR-452511, LLNL (2010).
[27] K. Shibata *et al.*, J. Nucl. Sci. Technol. **39**, 1125 (2002).
[28] R. Vanderbosch and J. R. Huizenga, *Nuclear Fission* (Academic Press, New York, 1973).
[29] G. Audi, A. H. Wapstra, and C. Thibault, Nucl. Phys. A **729**, 337 (2003).
[30] E. Browne and J. K. Tuli, Nucl. Data Sheets **108**, 681 (2007).
[31] E. Browne and J. K. Tuli, Nucl. Data Sheets **107**, 2649 (2006).